Downscaling Geostationary Land Surface Temperature Imagery for Urban Analysis

Iphigenia Keramitsoglou, *Member, IEEE*, Chris T. Kiranoudis, and Qihao Weng, *Member, IEEE*

***Abstract*—Although Earth observation data have been used in urban thermal applications extensively, these studies are often limited by the choices made in data selection, i.e., either using data with high spatial and low temporal resolution, or data with high temporal and low spatial resolution. The challenge of advancing the low spatial (3–5 km) resolution of geostationary land surface temperature (LST) images to 1 km—while maintaining the excellent temporal resolution of 15 min—is approached in this letter. The downscaling was performed using different advanced regression algorithms, such as support vector regression machines, neural networks, and regression trees, and its performance was improved using gradient boosting. The methodologies were tested on Meteosat Second Generation (MSG) SEVIRI LST images over an area of 19 600 km^2 centered in Athens, Greece. The output 1-km downscaled LST images were assessed against coincident LST maps derived from the thermal infrared imagery of the Moderate Resolution Imaging Spectroradiometer, the Advanced Very High Resolution Radiometer, and the Advanced Along Track Scanning Radiometer. The results showed that support vector machines coupled with gradient boosting proved to be a robust high-performance methodology reaching correlation coefficients from 0.69 to 0.81 when compared with the other satellite-derived LST maps.**

***Index Terms*—Boosting, Earth observing system, support vector regression machines (SVR), temperature measurement, urban areas.**

I. Introduction

AS HUMANS alter the characteristics of the natural landscape in the urbanization process, they affect and impact local energy exchanges that take place within the atmospheric boundary layer. The impact may be of a local, a regional, or a global scale, depending on the size of the area affected by urbanization [1]. A good starting point to gain understanding of the effect of urbanization is to examine urban surface energy balance and its key parameters such as land surface temperature (LST) and emissivity. In urban climate and environmental studies, remotely sensed thermal infrared imagery has been extensively used to measure these parameters. These measurements provide essential data for analyzing urban thermal landscape patterns and their relationship with surface biophysical characteristics, assessing the surface urban heat island (SUHI) effect and relating LST with surface heat fluxes for characterizing landscape properties, patterns, and processes [2]. If the advantage of time-sequential observations of satellite sensors (and daytime and nighttime imaging) is considered, remote sensing data have great potential for studying the urban surface energy budget and the spatial pattern and temporal dynamics of urban thermal landscapes [2].

The LST distribution and the observed SUHIs have been studied [3] using mostly satellite sensors of coarse spatial resolution, such as Advanced Very High Resolution Radiometer (AVHRR) on board National Oceanic and Atmospheric Administration platforms or Moderate Resolution Imaging Spectroradiometer (MODIS) on board Terra and Aqua satellites. At medium spatial resolution ($\sim$100 m), Thematic Mapper (TM) and Enhanced Thematic Mapper Plus (ETM+) on Landsat-5 and Landsat-7, respectively, and the Advanced Spaceborne Thermal Emission and Reflection Radiometer (ASTER) on Terra provide sparse "snapshots" of the LST distribution due to the eight-day repeat cycle when both satellites were operational; however, these images provide a valuable insight into local-scale hot spots, which is particularly important to city planners. Nevertheless, their use in generating higher level products, such as time evolution of SUHIs and heat wave hazard zones delineation within a city, is limited. The geostationary-orbit thermal infrared sensors provide images of the Earth's disk from 36 000 km every 15 to 30 min, making them unique means for capturing the diurnal variability of SUHIs; however, their spatial resolution of 3–5 km has prohibited their extensive use for urban studies. Sharpening (downscaling) the geostationary LST maps to finer resolution is worth investigating as the results combine the spatial resolution of 1 km with a temporal resolution of 15 min and thus open the prospect of numerous applications. Generally, downscaling is the enhancement of the spatial resolution of the original LST data set using ancillary information layers of superior spatial resolution. In practice, a coarse-resolution image is merged with a higher resolution image, so that the image of low resolution obtains the spatial details of the image with superior resolution [4]. Physical LST downscaling based on the dual-band method is often used in thermal anomaly monitoring [5]. With this method, one can estimate the percentage of a pixel covered by a thermal anomaly and its temperature. However, the method gives no solution on the position of the anomaly. Another physical approach assumes that the data to be downscaled are isothermal; thus, one can estimate subpixel emissivity and, afterward, subpixel LST, iteratively [6].

Statistical downscaling is also feasible based on the correlation between LST and other independent data, e.g., topography,

Manuscript received February 4, 2013; revised March 11, 2013; accepted March 29, 2013. Date of publication May 1, 2013; date of current version June 13, 2013.

I. Keramitsoglou is with the Institute for Astronomy, Astrophysics, Space Applications and Remote Sensing, National Observatory of Athens, GR15236 Athens, Greece (e-mail: ik@noa.gr).

C. T. Kiranoudis is with the School of Chemical Engineering, National Technical University of Athens, GR15780 Athens, Greece (e-mail: kyr@chemeng.ntua.gr).

Q. Weng is with the Center for Urban and Environmental Change, Department of Earth and Environmental Systems, Indiana State University, Terre Haute, IN 47809 USA (e-mail: qweng@indstate.edu).

Color versions of one or more of the figures in this paper are available online at http://ieeexplore.ieee.org.

Digital Object Identifier 10.1109/LGRS.2013.2257668

TABLE I
CHARACTERISTICS OF THE DATA SETS USED

Dataset reference	Dataset name	# images used and dates	Spatial Resolution	Used as	Source
A	MSG LST	480 (19-23/7/09)	3 km x5 km	Input	Generated and disseminated by the Land Surface Analysis Satellite Applications Facility (http://landsaf.ipma.pt/)
B	Corine Land Cover	1	Vector dataset	Input	European Environmental Agency (http://www.eea.europa.eu/)
C	Digital Terrain Model	1	$8.3x10^{-4}$° latitude, longitude	Input	Shuttle Radar Topography Mission (SRTM; http://srtm.usgs.gov/)
D	Vegetation indices	1 (12/7/2009)	1km	Input	MODIS global MOD13A2, 16-day average starting at the date stated
E	Emissivity	1 (22/7/2009)	1km	Input	MODIS global MOD11A1
F	AVHRR LST	7 (20-23/7/09)	1km	Assessment	Urban Heat Islands and Urban Thermography project (21913/08/I-LG) funded by the European Space Agency
G	AATSR LST	2 (21/7/09)	1km	Assessment	
H	MODIS LST	16 (20-23/7/2009)	1km	Assessment	MODIS MOD11A1and MYD11A1 daily products

vegetation cover and index, urban cover, emissivity, and other factors [7]–[9]. In the past, many approaches used the negative correlation between LST and the normalized difference vegetation index (NDVI) for LST downscaling purposes [10]–[12]. The NDVI cannot explain all the variation in LST; thus, it has been proposed [13] to enhance the results using the temperature difference between photosynthetically and nonphotosynthetically active vegetation. It is also possible to employ land cover data. In [14], the vegetation fraction from ETM+ images was derived, and a stronger negative correlation than the one between LST and NDVI was found. Emissivity and season-coincident LST were found to be also well correlated to the measured LST [4]. Many auxiliary data sets were combined in [15]: Leaf area index, NDVI, soil water content index, and reflectance of visible and near-infrared bands. To find the optimal downscaling solution, Yang *et al.* [15] employed an artificial neural network (NN) and tested their approach by downscaling aggregated ASTER data. Successful sharpening of geostationary LST maps with a spatial resolution of 3 km and a temporal resolution of 15 min would be equivalent to the maps with a spatial resolution of 1 km and a temporal resolution of 15 min, which is adequate for capturing the diurnal variability of SUHI and for input into urban climate models. Very recently, it has been showed that a spatial improvement by a factor of 2000 is possible [8], demonstrating the great potential in this field, yet using simple linear regression.

This letter investigates the potential of advanced regression methodologies, namely Support Vector Regression (SVR) machines, NNs, and regression trees (RTs) for downscaling geostationary LST imagery down to a spatial resolution of 1 km. The strength of the regression was improved using sophisticated gradient boosting techniques. The different methodologies (see Section II) were applied to Greater Athens Area, Greece. The comparative analysis is presented in Section III. The conclusions of our approach are drawn in Section IV.

II. DATA AND METHODS

A. Study Area

The study area is the Athens Greater Area. Athens is the capital and largest city of Greece. It has a population of approximately 4 000 000. The area lies at the southeasternmost edge of the Greek mainland. Athens sprawls across a central basin, bisected by a series of small hills, and bound by four mountains. The Saronic Gulf is in the southwest of Athens. Athens is a coastal city in a complex terrain, and these features make it particularly challenging for urban heat island and thermal pattern studies.

B. Data

The development, implementation, and assessment of the methodologies required a number of spatial data sets, which are summarized in Table I. The geostationary input data sets (Data set A) were acquired from the Spinning Enhanced Visible and Infrared Imager (SEVIRI) on board Meteosat Second Generation (MSG). MSG is at 36 000 km above point with 0° latitude and 0° longitude. SEVIRI has twelve spectral channels, eight of which are in the thermal infrared. The Land Surface Analysis Satellite Applications Facility (LSA SAF; https://landsaf.ipma.pt/) produces operationally LST maps [16]. The MSG LST product is computed within the area covered by the MSG disk, over four specific geographical regions (Europe, North Africa, South Africa, and South America) every 15 min. For each time slot and geographical region, the LST field and the respective quality control data are generated and disseminated through LSA SAF.

Finer spatial resolution input data sets ("components" hereafter) included Corine land cover vector data set (data set B), topography (data set C), and seasonally changing parameters (data sets D and E). Satellite-derived LST data sets from low Earth orbiters at a spatial resolution of 1 km (data sets F, G, and H) were used for assessing the results of downscaling. These data did not enter the calculations; they were used exclusively as additional information for the assessment of the proposed approaches.

C. Methods

1) Downscaling: We were inspired by the underlying principle of [7] and [8] but used different regression methodologies to produce downscaled 1 km/15′ LST data sets. The value ranges of the data sets (components) with fine spatial resolution differed largely by orders of magnitude (e.g., elevation from 0

to 1600 m, NDVI from -1 to 1); therefore, they were min–max normalized between -1 and 1 for integration in the regression models, so that all components had comparable values. The land cover data set (thematic information) was decomposed to provide percentages (numeric information) of certain land cover classes within a pixel of 1 km. We considered urban, agricultural land, vegetation, and water land cover classes [7]. For instance, one pixel could comprise of 70% urban, 0% agricultural, 20% vegetation, and 10% water. The same input data sets of Table I were used in all models for appropriate comparison of the results. The digital terrain model (data set C) was resampled to a 1-km grid using bilinear convolution to minimize discontinuities, which are not physically realistic. The selection of a pixel size of 1 km was driven by the available assessment data sets (data sets F, G, and H) and MODIS products (D and E).

2) Regression Models: Single image downscaling was conceived as three sequential phases. First, upscaling was performed to components, and a new set was derived at the geostationary LST image geometry (coarse resolution of $\sim$3 km). The second step was the core of downscaling and referred mainly to the development of the regression model. For each input LST coarse-resolution image, a unique regression model was defined. Computational intelligence models are attractive as they are data-driven models without *a priori* assumptions on their structure, permitting approximations of linear or nonlinear functions. The following popular state-of-the-art machine learning software libraries, all in the form of open source code, were used:

1) SVR LIBSVM, which is a library for SVMs [17] appropriate for classification, regression, and distribution estimation (available at http://www.csie.ntu.edu.tw/~cjlin/libsvm/);
2) SVR Light SVM [18], which is an implementation of SVMs for the problem of regression and for the problem of learning a ranking function (http://svmlight.joachims.org/);
3) Accord.NET SVM, a library for support vector machines that offers multiclass and multilabel implementations (http://code.google.com/p/accord/);
4) Accord.NET NNs, which is a library that involves parallel resilient back-propagation learning with Nguyen–Widrow [19] initialization procedures (http://code.google.com/p/accord/);
5) OpenCV RT algorithms utilizing decision trees as binary trees. For regression, a constant is assigned to each tree leaf; therefore, the approximation function is piecewise constant [20] (http://www.opencv.org/).

A significant advantage of SVMs over NNs is that, while the latter can suffer from multiple local minima, the solution to an SVM is global and unique. Additionally, SVMs have a simple geometric interpretation and reduce overfitting. RT is the weakest regression model of all that are used here but are considerably boosted using gradient boosting [20], [21].

The third step was the application of the regression model to the fine-scale components for the generation of the 1-km LST map.

3) Gradient Boosting: Boosting was introduced in the machine learning community as a concept that combined the predictions from one or even a collection of regression models in such a way that they form a much stronger regression model. As a result, boosting an SVR model for instance produces results of extreme quality when compared with predictions of the model itself. The most popular form of boosting is an additive formula that combines models such as NNs, generalized linear models, multivariate adaptive regression splines, wavelets, and classification trees and RTs. These models are appropriately weighted so that a loss function involving residuals from experimental data is minimized. Friedman [21] devised gradient boosting, which is an approximation technique that applies the method of steepest descent to forward stagewise estimation involving a two-step approximation of the loss function; the first step estimates parameters of each regression model using a least squares approach, and the second estimates the weights of the final additive function [21], [22]. In this letter, the boosted models were developed and trained with the coarse-resolution data sets and were then applied to the same components at 1 km to produce the downscaled LST image at 1 km. The combinations were B-SVR LIB SVM (gradient boosting using SVR LIB SVM model), B-SVR Light SVM, B-Accord.NET SVM, B-Accord.NET NN, and B-OpenCV RT.

4) Assessment of the Result: Assessment of the methodology adapted was carried out at two stages: first by comparing the LST image predicted by the regression models at a coarse scale against the original MSG coarse-resolution image (this step was applicable to all images), and subsequently, by comparing the final fine-resolution LST image against coincident MODIS, AVHRR, or Advanced Along-Track Scanning Radiometer LST maps (see Table I; this step was applicable only to geostationary images that could be paired with low-Earth-orbit products). The latter were selected for having the same spatial resolution (1 km) as the downscaled maps. Nevertheless, the angular configuration of the sensor, the sun, and the areas being measured have to be considered when interpreting the differences as sunlit and shaded areas of the same land cover will have different surface temperatures. Daytime and nighttime images were used. The comparison of both stages was carried out on a pixel-to-pixel basis by means of correlation coefficients (r_c^2 and r_f^2, for coarse- and fine-scale comparison, respectively), scatter plots, and maps of the differences between modeled and measured LST. Gradient boosting improved the result by an average of more than 15%.

III. Results

Downscaling of MSG LST images using advanced regression methodologies was applied to Athens, Greece, to reveal the diurnal dynamics of LST distribution. The most interesting results are presented in the following. As a rule, the thermal environment of Athens [23] during daytime depends on the cumulative influence of land cover and topography. Surfaces covered with sparse low vegetation such as olive trees or vineyards, and industrial zones and bare soils become warm faster than dense urban areas since concrete and asphalt are materials of high thermal inertia. The surrounding mountains exhibit lower surface temperatures. The situation is reversed during the nighttime, when higher LSTs are related with the residential urban zones. A dominant SUHI affects a number of central municipalities.

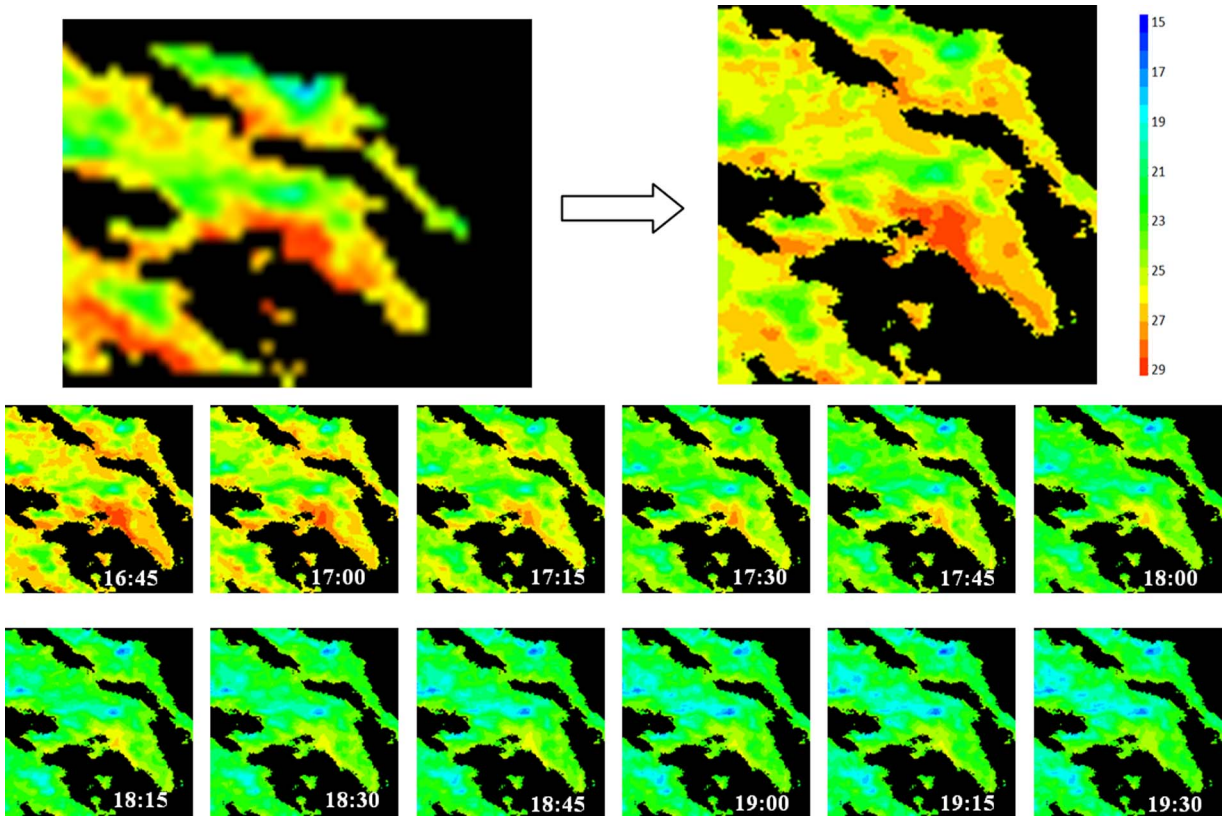

Fig. 1. Downscaling of the LST image in Athens, Greece. The top row shows the improvement in spatial resolution: (left) The original MSG LST map and (right) the downscaled map are presented for comparison. The next two rows show the evolution of SUHIs in Athens, Greece, which are seen for the first time at a temporal resolution of 15 min (Time in UTC) and a spatial resolution of 1 km on July 22, 2009.

TABLE II
COMPARATIVE ANALYSIS OF DIFFERENT REGRESSION METHODS. CORRELATION COEFFICIENTS ARE MULTIPLIED BY 100. ALL IMAGES ARE FROM JULY 22, 2009. LINEAR FIT WAS APPLIED TO IMAGE WINDOWS, THE REST REFER TO APPLICATION TO THE ENTIRE SCENE

	Assessment Image (reference to Dataset of Table I)	B-SVR-LIB SVM		B-SVR Light SVM		B- SVR Accord SVM		B-NN		B-RT		Linear fit	
Time UTC		r_c^2	r_f^2	r_c^2	r_f^2	r_c^2	r_f^2	r_c^2	r_f^2	r_c^2	r_f^2	r_c^2	r_f^2
2:30	MODIS (H)	83	78	80	**79**	85	76	84	**79**	95	75	81	75
8:00	AVHRR (F)	78	**69**	75	**69**	84	**69**	82	68	94	62	72	60
10:15	MODIS (H)	79	70	75	72	83	**74**	82	70	95	65	71	73
13:30	MODIS (H)	75	**73**	73	71	82	71	80	71	94	65	67	65
19:15	AVHRR (F)	85	78	82	**81**	88	77	85	78	95	79	75	72
21:30	MODIS (H)	83	69	81	74	86	71	84	**76**	96	**76**	70	71

A. Downscaling of MSG-SEVIRI

Fig. 1 shows the value of the proposed downscaling approach by introducing a novel insight into the diurnal dynamics of the SUHI in Athens at a spatial resolution of 1 km. The downscaled LST images in Fig. 1 were drawn at a 15-min step. The color scale used was common for all maps for better appreciation of the fade out of the SUHI pattern from 16:45 UTC (right after sunset) until 19:30 UTC. The highest LST was located at the city center at the beginning of the time sequence presented here. The Low coincides with the surrounding mountains. The results shown are for the images of July 22, 2009, using B-SVR Light SVM.

B. Comparative Analysis of Different Regression Models

The geostationary LST maps of one day (July 22, 2009) were downscaled using the different regression methods enhanced by gradient boosting. A comparative analysis revealed the advantages and drawbacks of each methodology for this application. Table II shows the correlation coefficients for coarse- and fine-scale comparisons (r_c^2 and r_f^2, respectively).

Table II presents the results of all regression methodologies discussed in Section II and of the window-based linear fit [7]. In bold are the highest correlation coefficients at fine scale (r_f^2) per image. The advanced regression algorithms were applied to the entire image circumventing the limitation of

local dependence of the linear regression equation. The former was found to result in higher scores than the latter. In three out of the six images considered here, B-SVR Light SVM was the one with the highest performance in the fine scale, depicted by the high correlation coefficients and visual assessment of the result for consistency in the output. In general, SVR machines produced comparable results and stability in solutions. B-RT resulted in a coarse correlation coefficient of 0.94 or higher in all cases; however, the fine-scale assessment revealed weaknesses in overall performance and in stability and coherence of the result. Stability in the solution, which is unique per image, is important for subsequent use of the downscaled data sets in 3-D visualization, extraction of thermal patterns, etc.

It has to be stressed that proper validation of LST maps derived from two different sensors cannot be carried out even if they are acquired at the same time. In particular, the different instantaneous fields of view, resulting in different pixel sizes, constrain the analysis of the differences between them. However, the only available resource of synchronous measurements were sensors on board low-Earth-orbit satellites; therefore, they were used to assess the result. Nighttime results were in better agreement than daytime ones. In addition, more conclusions can be drawn from the comparison between global SVR and local moving window linear regression. The two different approaches have comparable assessment scores (see Table II), but the global SVR depicts better the thermal patterns than the linear regression model. Furthermore, the former efficiently deals with scattered clouds by filling in the data gaps, whereas with the latter, the cloudy pixels are retained as gaps. The inland water bodies cause errors in the linear regression model [7], which is not the case with the global SVR. Finally, the coastline is retained in the downscaled image with the global SVR, whereas it is smoothed out with the local moving window approach; this is particularly important for coastal cities, such as Athens.

IV. Conclusion

This letter has presented advanced regression methodologies addressing efficiently the issue of downscaling LST products from geostationary satellites from a spatial resolution of $\sim$3 km to 1 km at a regional scale, allowing the study of the diurnal dynamics of the urban thermal environment, most notably the development and fade out of the SUHI. The main innovation of the approach presented in this letter over recent publications [7] is that the regression algorithms have been applied globally to the entire image by directly using a set of physically meaningful "components," thus circumventing: 1) principal components analysis; 2) the limitation of applying linear fit equations between LST and principal components, which is often not the case; 3) the local moving window and the resultant multiple linear regression models; 4) local clouds; and 5) errors of previous methods near large water bodies. For coastal cities, the latter is of decisive importance. The proposed methods have characteristics suitable for continental implementation: open-source libraries, state-of-the-art computing, integration of freely available global data sets, and fast execution times.

References

[1] Q. Weng, "Remote sensing of urban biophysical environments," in *Advances in Environmental Remote Sesning: Sensors, Algorithms, Applications*, Q. Weng, Ed. Boca Raton, FL, USA: CRC Press, 2011, pp. 503–523.

[2] Q. Weng, "Thermal infrared remote sensing for urban climate and environmental studies: Methods, applications, and trends," *ISPRS J. Photogramm. Remote Sens.*, vol. 64, no. 4, pp. 335–344, Jul. 2009.

[3] C. J. Tomlinson, L. Chapman, J. E. Thornes, and C. Baker, "Remote sensing land surface temperature for meteorology and climatology: A review," *Meteorol. Appl.*, vol. 18, no. 3, pp. 296–306, Sep. 2011.

[4] M. Stathopoulou and C. Cartalis, "Downscaling AVHRR land surface temperatures for improved surface urban heat island intensity estimation," *Remote Sens. Environ.*, vol. 113, no. 12, pp. 2592–2605, Dec. 2009.

[5] J. Dozier, "A method for satellite identification of surface temperature fields of subpixel resolution," *Remote Sens. Environ.*, vol. 11, pp. 221–229, 1981.

[6] D. Liu and R. Pu, "Downscaling thermal infrared radiance for subpixel land surface temperature retrieval," *Sensors*, vol. 8, no. 4, pp. 2695–2706, Apr. 2008.

[7] K. Zakšek and K. Oštir, "Downscaling land surface temperature for urban heat island diurnal cycle analysis," *Remote Sens. Environ.*, vol. 117, pp. 114–124, Feb. 2012.

[8] B. Bechtel, K. Zakšek, and G. Hoshyaripour, "Downscaling land surface temperature in an urban area: A case study for Hamburg, Germany," *Remote Sens.*, vol. 4, no. 10, pp. 3184–3200, Oct. 2012.

[9] I. Keramitsoglou, "Advanced earth observation methodologies for the study of the thermal environment of cities," in *Proc. 2nd Int. Workshop EORSA*, 2012, pp. 11–15.

[10] W. P. Kustas, J. M. Norman, M. C. Anderson, and A. N. French, "Estimating subpixel surface temperatures and energy fluxes from the vegetation index-radiometric temperature relationship," *Remote Sens. Environ.*, vol. 85, no. 4, pp. 429–440, Jun. 2003.

[11] N. Agam, W. P. Kustas, M. C. Anderson, F. Li, and C. M. Neale, "A vegetation index based technique for spatial sharpening of thermal imagery," *Remote Sens. Environ.*, vol. 107, no. 4, pp. 545–558, Apr. 2007.

[12] A. K. Inamdar, A. French, S. Hook, G. Vaughan, and W. Luckett, "Land surface temperature retrieval at high spatial and temporal resolutions over the southwestern United States," *J. Geophys. Res.*, vol. 113, no. D7, p. D07 107, 2008.

[13] O. Merlin, B. Duchemin, O. Hagolle, F. Jacob, B. Coudert, G. Chehbouni, G. Dedieu, J. Garatuza, and Y. Kerr, "Disaggregation of MODIS surface temperature over an agricultural area using a time series of Formosat-2 images," *Remote Sens. Environ.*, vol. 114, no. 11, pp. 2500–2512, Nov. 2010.

[14] Q. Weng, D. Lu, and J. Schubring, "Estimation of land surface temperature-vegetation abundance relationship for urban heat island studies," *Remote Sens. Environ.*, vol. 89, no. 4, pp. 467–483, Feb. 2004.

[15] G. Yang, R. Pu, W. Huang, J. Wang, and C. Zhao, "A novel method to estimate subpixel temperature by fusing solar-reflective and thermal-infrared remotesensing data with an artificial neural network," *IEEE Trans. Geosci. Remote Sens.*, vol. 48, no. 4, pp. 2170–2178, Apr. 2010.

[16] I. F. Trigo, C. C. DaCamara, P. Viterbo, J.-L. Roujean, F. Olesen, C. Barroso, F. Camacho-de Coca, D. Carrer, S. C. Freitas, J. García-Haro, B. Geiger, F. Gellens-Meulenberghs, N. Ghilain, J. Meliá, L. Pessanha, N. Siljamo, and A. Arboleda, "The satellite application facility on land surface analysis," *Int. J. Remote Sens.*, vol. 32, no. 10, pp. 2725–2744, May 2011.

[17] C.-C. Chang and C.-J. Lin, "LIBSVM: A library for support vector machines," *ACM Trans. Intell. Syst. Technol.*, vol. 2, no. 3, pp. 27:1–27:27, Apr. 2011.

[18] T. Joachims, *Learning to Classify Text Using Support Vector Machines: Methods, Theory and Algorithms*. Norwell, MA, USA: Kluwer, 2002, ser. The Springer International Series in Engineering and Computer Science.

[19] D. Nguyen and B. Widrow, "Improving the learning speed of 2-layer neural networks by choosing initial values of the adaptive weights," in *Proc. Int. Joint Conf. Neural Netw.*, 1990, vol. 3, pp. 21–26.

[20] L. Breiman, J. Friedman, R. Olshen, and C. Stone, *Classification and Regression Trees*. Belmont, CA, USA: Wadsworth Int. Group, 1984.

[21] J. H. Friedman, "Greedy function approximation: A gradient boosting machine," *Ann. Stat.*, vol. 29, no. 5, pp. 1189–1232, Oct. 2001.

[22] T. J. Hastie, R. J. Tibshirani, and J. H. Friedman, *The Elements of Statistical Learning*. NY, NY, USA: Springer-Verlag, 2001.

[23] I. Keramitsoglou, C. T. Kiranoudis, G. Ceriola, Q. Weng, and U. Rajasekard, "Identification and analysis of urban surface temperature patterns in greater Athens, Greece, using MODIS imagery," *Remote Sens. Environ.*, vol. 115, no. 12, pp. 3080–3090, Dec. 2011.